



## An Observer based Open-Circuit Fault Detection for Switches of PMSM Drive

A. Pawan Sai Kumar ; Sruthi Mahapatro ; S.Suvarna ; T.Jyothsna ; Y.Deepthikala

(Electrical And Electronics Engineering)

**Abstract**—This work describes a simple and economical technique for locating and diagnosing malfunctions in the open circuit of voltage-source inverters (VSIs) when they are utilized with permanent magnet synchronous motors (PMSM) that are pulse-width modulated (PWM). Phase-by-phase voltage distortions and changes in the terminal voltage are the results of PWM VSI power switch open-circuit faults. By using model reference adaptive system techniques, the suggested fault detection method can identify the broken switch and detect problems without the need for further sensors or electrical equipment. This approach is noteworthy because it provides quick diagnosis, a straightforward structure, and simple integration as a subroutine with little modification into current control algorithms. Experiments and simulations show that the suggested method works well.

### INTRODUCTION

The motor that runs on permanent magnets (PMSM) finds application in a growing number of industries, such as electric vehicles, powered wheelchairs, nuclear power plants, aerospace, medical, and military. This is because of its many benefits, including its efficiency, ease of control, torque to inertia ratio, and high po density. In these applications, machine drive dependability is critical because of the possibility of errors or accidents that could cause serious harm to both the environment and human life. In the event of an emergency or malfunction, the drive system frequently needs to be shut down right away for emergency repairs. There is an increasing interest in creating dependable systems that can run continuously and safely even in the event of a malfunction, given the high expense of unplanned repair.

The three functions of fault detection, problem identification, and corrective measures are usually involved in a fault-tolerant control system, which reduces or eliminates the impacts of faults. When it comes to actual application, fault diagnosis refers to the combination of these tasks that are especially important for defect detection and identification. The power electronic converter (PWM VSI, or pulse-width modulated voltage-source inverter) is used in the majority of motor drive systems serves as the brains behind the control algorithms, while the motor itself is the last component. Subsystems and individual parts such as the MCU, motor, power converter, sensors, connectors, and wires

are all susceptible to malfunctions. That being said, as compared to other system components, Generally, the MCU, wires, and connections have low failure rates. The high maintenance costs associated with power converter failures, especially in PWM VSI power switches, are a major risk factor and can cause system shutdowns.

A power electronic converter, also known as a pulse-width modulated voltage source inverter (PWM VSI), a motor, and a microcontroller unit (MCU) for executing control algorithms are the typical components of motor drive systems. Various fault types can arise in the following components.

- 1.The microcontroller unit (MCU)
2. PMSM (permanent magnet synchronous motor)
- 3.PWM(volt-state-inverter)
4. Sensors: position encoder, voltage and current
5. Wires and connectors.

Comparing the mcu, cables, connectors to the rest of the system, the failure rates are incredibly low. This is due to the MCU's high level of dependability and lack of high voltages or currents. When chosen and installed correctly, the static connections and cables have low failure rates. Certain machine faults caused by winding insulation failure due to their excessive voltage or current stress can virtually be eliminated because line voltage surges are absorbed at the power converter's input side and current stresses are

limited by the power converter's overcurrent protection.

Open-circuit faults, which have slower response times and less immediate damage to the drive system, should not be disregarded, even if short-circuit failures are frequently given priority because of their immediate danger. Heat cycling or gate driver malfunctions can cause wire disconnections from switching devices, leading to open-circuit issues. Open-circuit failures can result in decreased driving performance and possibly even secondary faults in other components, even though they usually do not cause system shutdowns. The diagnosis of open-circuit failures in motor drive systems has been the focus of a lot of research efforts. The complexity and efficacy of currently available approaches differ; some require extra hardware or complex algorithms, which raises system costs and complexity.

In this research, an open-circuit fault diagnostic algorithm for PWM VSIs in PMSM drives is proposed, which is both simple and economical. This technique delivers quick, easy, and affordable features while doing away with the need for extra sensors. Its foundation is the PWM VSI analytical model. It requires little modification to be smoothly incorporated into current drive systems. The proposed method is validated by simulations and experiments and is implemented digitally with an MCU TMS320F28335 from Texas Instruments, Incorporated.

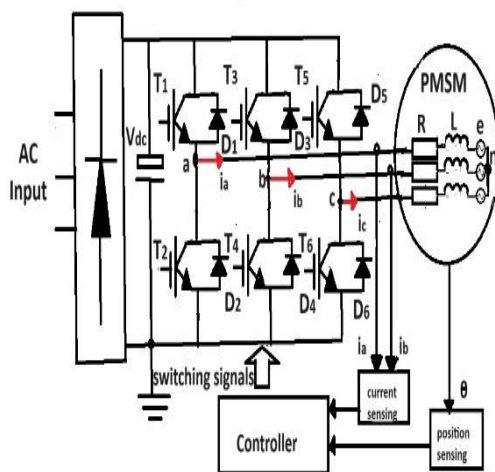


Fig. 1. PMSM drive system.

## I. OPEN CIRCUIT FAULT ANALYSIS

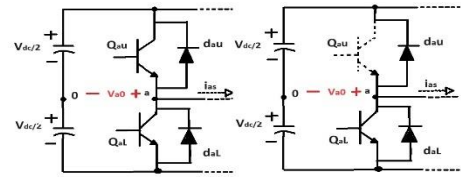


Fig. 2. Phase diagram basic configuration a three-phase PWM VSI's leg(a) Typical state. (b) The upper switch QaU has an open circuit problem.

Fig. 2 shows the basic configuration of the phase A leg of a three-phase PWM VSI. The terminal voltage of phase A,  $v_{a0}$ , is defined by the phase current,  $i_{as}$ , and the switching function,  $S_a$ , of QaU and QaL, when the system is functioning correctly, as shown in Fig. 2(a). If the switching function is 1, then the terminal voltage of phase A is equal to  $V_{dc}/2$ , where  $V_{dc}$  is the dc-link voltage and QaU is turned ON and QaL is turned OFF. When the switching function is 0,  $v_{a0} = -V_{dc}/2$  signals that QaU is switched off and QaL is turned on.

TABLE 1

Phase A terminal voltages under normal conditions

	$S_a = 1$	$S_a = 0$
$i_{as} \geq 0$	$v_{a0} = \frac{V_{dc}}{2}$	$v_{a0} = -\frac{V_{dc}}{2}$
$i_{as} < 0$	$v_{a0} = \frac{V_{dc}}{2}$	$v_{a0} = -\frac{V_{dc}}{2}$

TABLE II

Phase A terminal voltages under open-circuit fault conditions

	$S_a = 1$	$S_a = 0$
$i_{as} \geq 0$	$v_{a0} = -\frac{V_{dc}}{2}$	$v_{a0} = -\frac{V_{dc}}{2}$
$i_{as} < 0$	$v_{a0} = \frac{V_{dc}}{2}$	$v_{a0} = -\frac{V_{dc}}{2}$

The corresponding terminal voltage changes when there is an open-circuit fault in the upper switch QaU, which occurs when the phase current is positive and the switching function is 1. The terminal voltage of phase A is equal to  $-V_{dc}/2$ . To properly investigate how an open-circuit defect of a switch impacts the phase voltages, one must have a thorough understanding of the relationship between the terminal voltages and the phase voltages.

$$\begin{bmatrix} v_{a0} \\ v_{b0} \\ v_{c0} \end{bmatrix} = \begin{bmatrix} v_{as} \\ v_{bs} \\ v_{cs} \end{bmatrix} + v_{s0} \quad (1)$$

where  $v_{s0}$  is the neutral to center voltage and  $v_{as}$ ,  $v_{bs}$ , and  $v_{cs}$  are the phase voltages. In a

three-phase, three-wire system, Kirchoff's law's specified requirement is met as

$$i_{as} + i_{bs} + i_{cs} = 0 \quad (2)$$

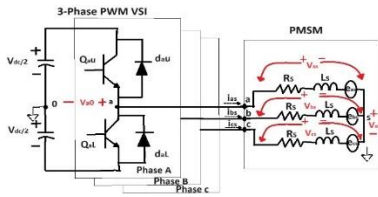


Fig. 3. Relationship between terminal voltages and phase voltages

Moreover, the total phase back EMF at any given moment equals 0 if the air-gap magnetic flux distribution is sinusoidal on average. Based on (2) and this presumption, the PMSM's subsequent requirements are satisfied.

$$v_{as} + v_{bs} + v_{cs} = R_s(i_{as} + i_{bs} + i_{cs}) + L_s \frac{d}{dt}(i_{as} + i_{bs} + i_{cs}) + (e_{as} + e_{bs} + e_{cs}) = 0 \quad (3)$$

where eas, ebs, and ecs stand for the appropriate phase back EMFs, and Rs, Ls, and eas, ebs, and ecs, respectively, are the stator resistance and inductance. The neutral to center voltage, vs0, changes from (1) to (3) to

$$v_{s0} = \frac{1}{3}(v_{a0} + v_{b0} + v_{c0}) \quad (4)$$

The following diagram illustrates the relationship between the phase and terminal voltages:

$$\begin{bmatrix} v_{as} \\ v_{bs} \\ v_{cs} \end{bmatrix} = \frac{1}{3} \begin{bmatrix} 2 & -1 & -1 \\ -1 & 2 & -1 \\ -1 & -1 & 2 \end{bmatrix} \begin{bmatrix} v_{a0} \\ v_{b0} \\ v_{c0} \end{bmatrix} \quad (5)$$

On the other hand, a deviation value from the PWM VSI terminal voltages can be used to depict the impact of an open-circuit problem on a single switch. Assuming that  $\Delta v_{a0}$  represents the voltage deviation resulting from an open-circuit fault in the upper switch  $Q_{aU}$ , the phase voltages following the occurrence of the open-circuit fault are represented as follows:

Conversely, the effect of an open-circuit issue on a single switch can be illustrated using a deviation value from the PWM VSI terminal voltages. The phase voltages after the open-circuit failure occur as follows, assuming that  $\Delta v_{a0}$  reflects the voltage deviation brought on by an open-circuit fault in the upper switch  $Q_{aU}$ :

$$\begin{bmatrix} v_{as_f} \\ v_{bs_f} \\ v_{cs_f} \end{bmatrix} = \frac{1}{3} \begin{bmatrix} 2 & -1 & -1 \\ -1 & 2 & -1 \\ -1 & -1 & 2 \end{bmatrix} \begin{bmatrix} v_{a0} - \Delta v_{a0} \\ v_{b0} \\ v_{c0} \end{bmatrix} \quad (6)$$

where  $v_{as_f}$ ,  $v_{bs_f}$ , and  $v_{cs_f}$  are the phase voltages after the open-circuit fault occurs to the upper switch  $Q_{aU}$ . After some calculations equation (6) can be expressed as

$$\begin{bmatrix} v_{as_f} \\ v_{bs_f} \\ v_{cs_f} \end{bmatrix} = \begin{bmatrix} v_{as} \\ v_{bs} \\ v_{cs} \end{bmatrix} + \frac{1}{3} \begin{bmatrix} -2\Delta v_{a0} \\ \Delta v_{a0} \\ \Delta v_{a0} \end{bmatrix} = \begin{bmatrix} v_{as} \\ v_{bs} \\ v_{cs} \end{bmatrix} + \begin{bmatrix} \Delta v_{as\_dist} \\ \Delta v_{bs\_dist} \\ \Delta v_{cs\_dist} \end{bmatrix} \quad (7)$$

where  $\Delta v_{as}$ ,  $\Delta v_{bs}$ , and  $\Delta v_{cs}$  indicate the phase voltage variations brought on by the higher switch  $Q_{aU}$ 's open-circuit failure. As can be seen in (7), there are two components to the phase voltage following the occurrence of the open-circuit fault: the normal phase voltages are represented by the first term of (7),  $\Delta v_{ks}$  ( $k = \{a,b,c\}$ ), and the voltage deviations caused by the open-circuit fault in the upper switch  $Q_{aU}$  are represented by the second term of (7),  $\Delta v_{ks\_dist}$  ( $k = \{a,b,c\}$ ), which are the voltage deviations caused by the open-circuit fault. These phase voltage abnormalities, which are seen from the machine characteristics and can be conceptualized as "voltage distortions" due to the open-circuit defect, are discussed in

$$\begin{bmatrix} v_{q\_f} \\ v_{d\_f} \end{bmatrix} = T(\theta_e) \begin{bmatrix} v_{as\_f} \\ v_{bs\_f} \\ v_{cs\_f} \end{bmatrix} \quad (8)$$

$$T(\theta_e) = \frac{2}{3} \begin{bmatrix} \cos \theta_e & \cos(\theta_e - \frac{2\pi}{3}) & \cos(\theta_e + \frac{2\pi}{3}) \\ \sin \theta_e & \sin(\theta_e - \frac{2\pi}{3}) & \sin(\theta_e + \frac{2\pi}{3}) \end{bmatrix} \quad (9)$$

where  $\theta_e$  represents the rotor's electrical angular position. The voltage distortions in the rotor reference frame in (8) can be expressed as follows by using (7) through (9).

$$\begin{bmatrix} v_{q\_f} \\ v_{d\_f} \end{bmatrix} = T(\theta_e) \begin{bmatrix} v_{as} + \Delta v_{as\_dist} \\ v_{bs} + \Delta v_{bs\_dist} \\ v_{cs} + \Delta v_{cs\_dist} \end{bmatrix} = \begin{bmatrix} v_q \\ v_d \end{bmatrix} + \begin{bmatrix} \Delta v_{q\_dist} \\ \Delta v_{d\_dist} \end{bmatrix} \quad (10)$$

Where  $v_q$  and  $v_d$  are the normal q- and d-axis values,  $\Delta v_{q\_dist}$  and  $\Delta v_{d\_dist}$  are the q- and d-axis voltage deviations or distortions caused by the open-circuit fault, and  $v_{q\_f}$  and  $v_{d\_f}$  are the q- and d-axis voltages after the fault. An alternative representation of the stator voltages could be two parts in the rotor reference frame after the issue occurs. There are two voltages at play: the normal q- and d-axis voltages as well as the voltage fluctuations caused by the open-circuit fault. The open-circuit failure in the remaining switches can be analyzed similarly.

### III. MRAS-Based Voltage Distortion Observer

The voltage distortions brought on by the open-circuit fault can be included in the current dynamics of a PMSM and shown as follows:

$$\begin{bmatrix} \frac{di_q}{dt} \\ \frac{di_d}{dt} \end{bmatrix} = \begin{bmatrix} -\frac{R_s}{L_s} & -\omega_e \\ \omega_e & -\frac{R_s}{L_s} \end{bmatrix} \begin{bmatrix} i_q \\ i_d \end{bmatrix} + \frac{1}{L_s} \begin{bmatrix} v_q + \Delta v_{q\_dist} \\ v_d + \Delta v_{d\_dist} \end{bmatrix} + \begin{bmatrix} -\frac{\lambda_m \omega_e}{L_s} \\ 0 \end{bmatrix} \quad (11)$$

where  $\omega_e$  is the electrical rotor angular speed,  $\lambda_m$  is the flux linkage produced by the permanent magnet, and  $i_q$  and  $i_d$  are the q- and d-axis currents, respectively. (11), which shows how the motor currents are affected by the voltage aberrations caused by the open-circuit failure.

In the MRAS reference model, it is assumed that the system is in the healthy state and that there are no voltage distortions associated to open-circuit faults. Another method to represent the estimated current dynamics in this scenario with the nominal parameters is as follows:

$$\begin{bmatrix} \frac{di_{qm}}{dt} \\ \frac{di_{dm}}{dt} \end{bmatrix} = \begin{bmatrix} -\frac{R_{s0}}{L_{s0}} & -\omega_e \\ \omega_e & -\frac{R_{s0}}{L_{s0}} \end{bmatrix} \begin{bmatrix} i_q \\ i_d \end{bmatrix} + \frac{1}{L_{s0}} \begin{bmatrix} v_q^* \\ v_d^* \end{bmatrix} + \begin{bmatrix} -\frac{\lambda_{m0} \omega_e}{L_{s0}} \\ 0 \end{bmatrix} \quad (12)$$

where the subscript "0" represents the nominal value and the variables  $i_{qm}$  and  $i_{dm}$  are the model's q- and d-axis currents, respectively.  $v_q^*$  and  $v_d^*$  stand for the q- and d-axis stator voltage instructions.

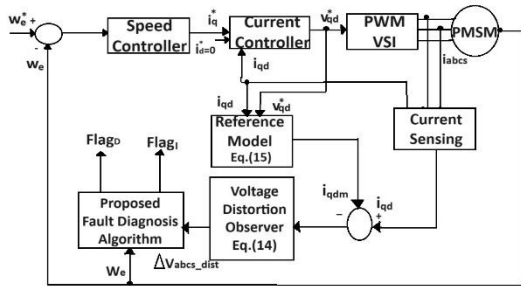


Fig. 4. Configuration of the proposed voltage distortion observer

The voltage distortions in the rotor reference frame resulting from the open-circuit fault can be determined as follows from equations (11) and (12):

$$\begin{aligned} \Delta v_{q\_dist} &= L_s \left( \frac{di_q}{dt} - \frac{di_{qm}}{dt} \right) \\ \Delta v_{d\_dist} &= L_s \left( \frac{di_d}{dt} - \frac{di_{dm}}{dt} \right) \end{aligned} \quad (13)$$

If it is assumed that the nominal parameters,  $R_{s0}$ ,  $L_{s0}$ , and  $\lambda_{m0}$ , correspond to the real values of  $R_s$ ,  $L_s$ , and  $\lambda_m$ . Furthermore, if the switches in the PWM VSI are flawless, the voltage commands  $v_q^*$  and  $v_d^*$  are the same as the matching q- and d-axis voltages  $v_q$  and  $v_d$ . The following method can be

used to calculate the average voltage distortions over the  $k$ th PWM step from (13)

$$\Delta v_{q\_dist}(k) = L_s \left( \frac{i_q(k) - i_{qm}(k)}{T_s} \right)$$

$$\Delta v_{d\_dist}(k) = L_s \left( \frac{i_d(k) - i_{dm}(k)}{T_s} \right) \quad (14)$$

The discrete version of (12) can be used to obtain the model currents  $i_{qm}(k)$  and  $i_{dm}(k)$  in (14) as follows:

$$\begin{aligned} i_{qm}(k) &= i_q(k-1) + \frac{T_s}{L_{s0}} [v_q^*(k-1) - R_{s0}i_q(k-1) - \omega_e L_{s0}i_d(k-1) - \omega_e \lambda_{m0}] \\ i_{dm}(k) &= i_d(k-1) + \frac{T_s}{L_{s0}} [v_d^*(k-1) - R_{s0}i_d(k-1) - \omega_e L_{s0}i_q(k-1)] \end{aligned} \quad (15)$$

Fig. 4 shows the block diagram for the proposed voltage distortion observer. The PWM VSI's open-circuit failure diagnostic algorithm is derived from model currents and plant-observed voltage aberrations. This proposed fault diagnostic system uses two strategies—error detection and fault detection time—to provide robustness against false fault diagnosis. Under typical operating conditions, the voltage distortions in (14) are zero. Conversely, in the event of a malfunction, the defective switch within the PWM VSI generates voltage distortions, which may exhibit either positive or negative values contingent upon the nature of the issue and recurrently transpire while the defective leg's current is zero. Therefore, the threshold value is utilized to determine the error occurrence, and it is given

$$V_{th} = K \quad (16)$$

where  $K$  is a deliberately selected positive integer intended to lower the probability of false alarms, which are primarily caused by sounds and less-than-ideal features of the power switches. In the previously described open-circuit fault analysis, it was believed that the switches were flawless, thus the voltage commands and the matching voltages applied to the PMSM are the same. Since they are not the same, there exist voltage differences between the voltage commands and the corresponding real applied voltages in a real situation. This phenomenon, known as the dead-time effect, is caused by the nonideal features of the switching devices and purposeful blanking time to prevent the arm-short of a switch leg. The voltage fluctuations resulting from the dead-time effect can be depicted as

$$v_{as}^{dead} = v_{as}^* - v_{as} \approx (2 \operatorname{sgn}(i_{as}) - \operatorname{sgn}(i_{bs}) - \operatorname{sgn}(i_{cs})) \cdot A_p$$

$$v_{bs}^{dead} = v_{bs}^* - v_{bs} \approx (2 \operatorname{sgn}(i_{bs}) - \operatorname{sgn}(i_{cs}) - \operatorname{sgn}(i_{as})) \cdot A_p$$

$$v_{cs}^{dead} = v_{cs}^* - v_{cs} \approx (2 \operatorname{sgn}(i_{cs}) - \operatorname{sgn}(i_{as}) - \operatorname{sgn}(i_{bs})) \cdot A_p$$

(17)

$$A_p = \frac{1}{6}(2(V_{dc} - V_{ce} - V_d) \frac{(t_{dead} + t_{on} - t_{off})}{T_s} + (V_{ce} + V_d)) \quad (18)$$

where  $T_s$  is the sample period,  $t_{dead}$  is the blanking time to prevent the short-circuit,  $t_{on}$  is the sum of the turn-on delay and transition time,  $t_{off}$  is the sum of the turn-off delay and transition time,  $V_{ce}$  is the saturation voltage of the active switch, and  $V_d$  is the forward voltage of the antiparallel diode. , one can choose the threshold value  $K$  in (16) by

$$K = m \cdot V_{max} \quad (19)$$

where  $V_{max}$  is the highest value of (17) and  $m$  is a positive number. This value was specifically selected to lower the possibility of inaccurate error detection due to dead-time effects and noise. If  $m$  is selected too high, it's possible that the flaws won't be discovered. Moreover, if  $m$  is too little, there is a higher likelihood of error detection. The following fundamental logic is applied to each phase during the observation of the voltage distortions in (14) during an open-circuit failure, producing the Boolean errors  $\epsilon_{ks}(k = \{a, b, c\})$  as

$$\epsilon_{ks} = \begin{cases} 1, & \Delta v_{ks\_dist} > V_{th} : error \\ 0, & |\Delta v_{ks\_dist}| < V_{th} : normal \\ -1, & \Delta v_{ks\_dist} < -V_{th} : error \end{cases} \quad (20)$$

where  $V_{th}$  is the threshold value selected in equations (16) through (19), and  $\Delta v_{ks\_dist}$  ( $k = a, b, c$ ) represents the voltage distortions detected in the abc frame.  $\epsilon_{ks}$  ( $k = a, b, c$ ) are the produced Boolean errors for each phase. A Boolean error of 1 or -1 in equation (20) suggests that the system might be in a fault condition. If the number of Boolean faults is zero, the system can be functioning normally. In addition to producing repetitive square waveforms when there is a problem, the voltage distortions also cause Boolean errors to repeatedly display either a positive or negative value, depending on which switch is failing. Thus, the fault condition can be determined by looking at the ensuing Boolean errors. The voltage distortions and ensuing Boolean errors caused by the broken switch are shown in Table IV. Table IV demonstrates that examining the resulting Boolean errors allows for the detection of both the fault condition and the faulty switch. Noise and operating point changes can lead to false positives even using the simple and frequently used error detection approach in (20). Given the duration of continuous Boolean error generation, the fault detection time  $T_{fault}$  is determined by

$$T_{fault} = k_f \cdot T_s \quad (21)$$

where  $k_f$  is the fault detection sensitivity factor and  $T_s$  is the sample time. If  $k_f$  is too big, the open-circuit fault could go unnoticed. When  $k_f$  is too low, there is a greater chance of incorrect detection. Because of this, the sensitivity factor,  $k_f$ , is carefully selected while accounting for the detection

time and fault detection reliability. The principles of error detection and fault detection time from equations (20) and (21) are used to give the fault detection technique.

$$Flag_D = \begin{cases} 1, & t_e \geq T_{fault} : fault \\ 0, & t_e < T_{fault} : normal \end{cases} \quad (22)$$

where  $t_e$  is the amount of time that has elapsed between the beginning of error detection in (20) and the arrival at the fault detection time  $T_{fault}$ , and  $Flag\_D$  is the fault detection flag indicating the fault state. The error detection time  $t_e$  is reset to zero when the Boolean errors have a value of zero. In terms of fault detection, the open-circuit fault is found when the fault detection time  $T_{fault}$ , which is described in equation (21) is shorter than the error detection time  $t_e$ . The fault detection flag  $Flag\_D$  is set from low to high if  $t_e$  is less than  $T_{fault}$ . When two of the three legs' switches are open-circuited

there is an open-phase fault. Section II allows for similar analysis, with the exception that the effect of the faulty switch on the voltage distortions appears in a different way. For example, when two switches in phase A,  $QaU$  and  $QaL$ , have open-circuit faults, the voltage distortions fluctuate between positive and negative values and between negative and positive values, depending on which switch is broken. The phase voltages after the occurrence of the open-circuit fault are displayed as follows in the case when the lower switch  $QaL$  experiences an open-circuit fault first:

$$\begin{bmatrix} v_{as\_f1} \\ v_{bs\_f1} \\ v_{cs\_f1} \end{bmatrix} = \frac{1}{3} \begin{bmatrix} 2 & -1 & -1 \\ -1 & 2 & -1 \\ -1 & -1 & 2 \end{bmatrix} \begin{bmatrix} v_{a0} + \Delta v_{a0} \\ v_{b0} \\ v_{c0} \end{bmatrix} = \begin{bmatrix} v_{as} \\ v_{bs} \\ v_{cs} \end{bmatrix} + \frac{1}{3} \begin{bmatrix} 2\Delta v_{a0} \\ -\Delta v_{a0} \\ -\Delta v_{a0} \end{bmatrix} \quad (23)$$

A further open-circuit fault in the higher switch  $QaU$  transpires after the lower switch  $QaL$  experiences one. Here is a representation of the phase voltages:

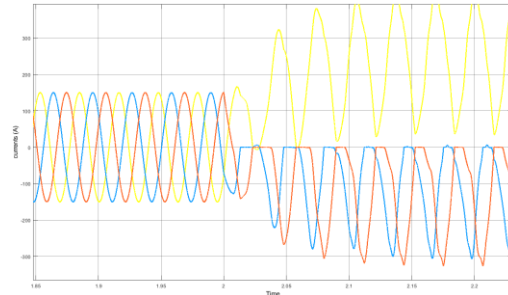
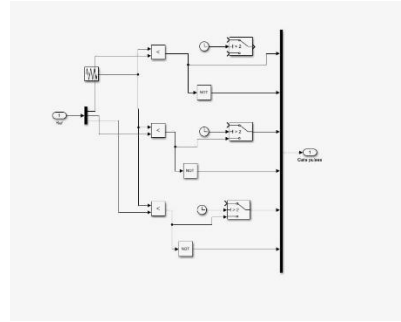
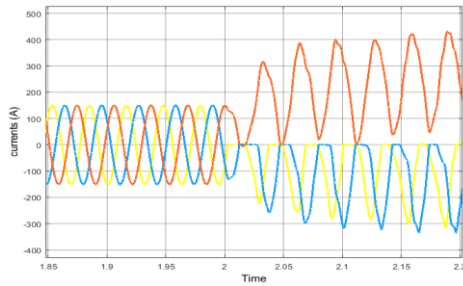
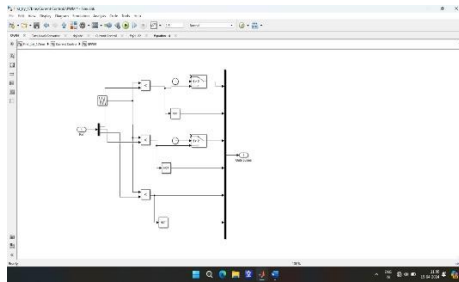
$$\begin{bmatrix} v_{as\_f2} \\ v_{bs\_f2} \\ v_{cs\_f2} \end{bmatrix} = \frac{1}{3} \begin{bmatrix} 2 & -1 & -1 \\ -1 & 2 & -1 \\ -1 & -1 & 2 \end{bmatrix} \begin{bmatrix} v_{a0} - \Delta v_{a0} \\ v_{b0} \\ v_{c0} \end{bmatrix} = \begin{bmatrix} v_{as} \\ v_{bs} \\ v_{cs} \end{bmatrix} + \frac{1}{3} \begin{bmatrix} -2\Delta v_{a0} \\ \Delta v_{a0} \\ \Delta v_{a0} \end{bmatrix} \quad (24)$$

Equations (23) and (24) show that the voltage distortions might have positive to negative or negative to positive values, depending on which switch is malfunctioning. The method previously mentioned can be used to identify the defective switch or leg.

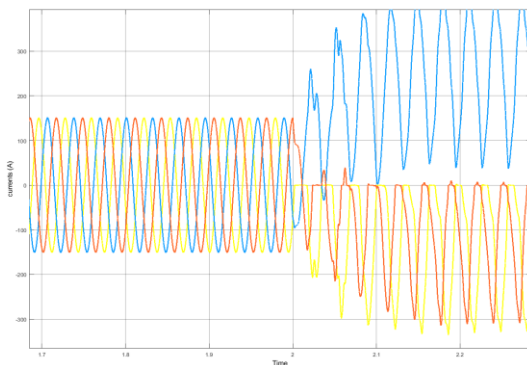
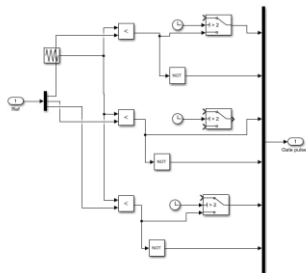
### Various Types of Open-Circuit

#### Faults in Switches:

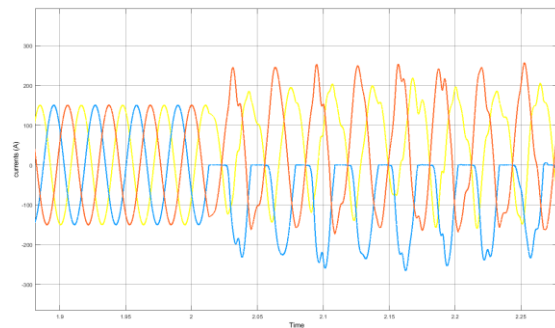
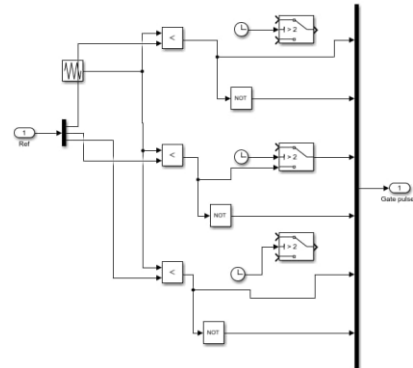
##### Fault (1)



##### Fault (2)

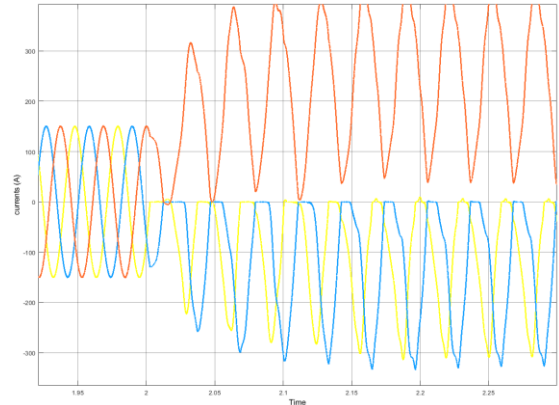
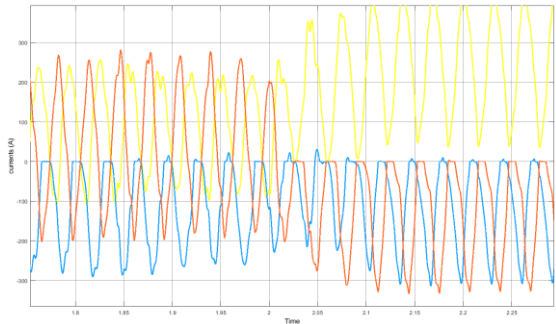
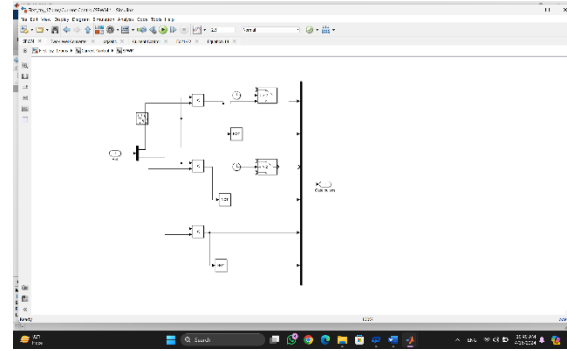
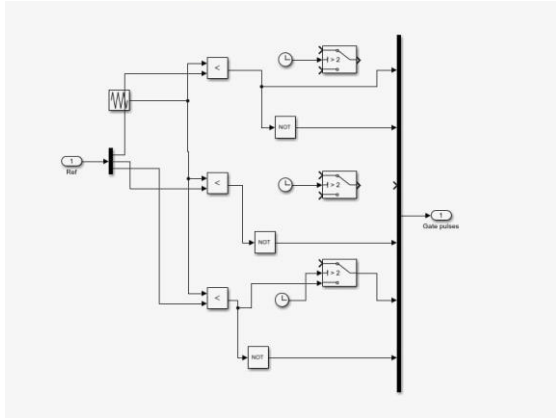


##### Fault (4)

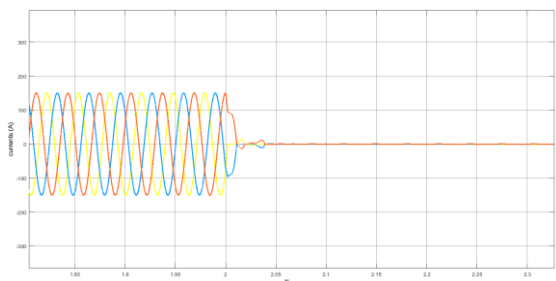
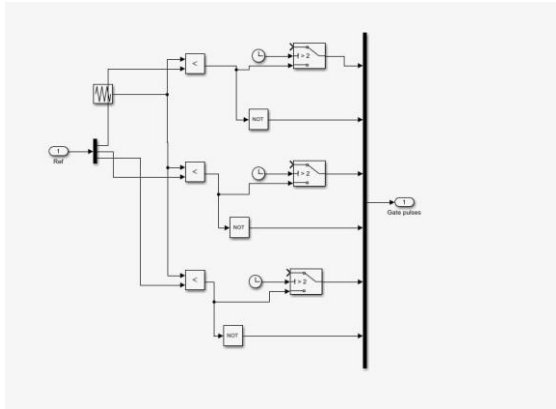


##### Fault (3)

##### Fault (5)



### Fault (6)



### Fault (7)

### Conclusion

The significance of defect detection and identification in industrial applications is steadily growing. Enhancing the fault diagnosis capabilities is therefore becoming more and more necessary. The open-circuit fault detection and identification technique describes in this research is straightforward and inexpensive. It is the basic voltage distortion observer that makes possible the suggested defect diagnosis. Following estimation of the voltage distortions, the fault status is ascertained by comparing them to the threshold value. There are voltage distortions that are seen that beyond the threshold value when an open-circuit failure happens. We determine the fault condition by comparing these two numbers. Because the voltage distortions vary depending on which switch is malfunctioning, it is also possible to identify faults by using the observed voltage distortions. The postfault actions, which involve reconfiguring the entire drive system to function safely and constantly, can be effectively paired with the suggested strategy. Nevertheless, the postfault behaviours are outside the purview of this



manuscript. The suggested approach has a straightforward structure and a quick fault identification time as compared to the prior fault diagnosis. Additionally, the computing effort is minimal and it may be accomplished without the need for additional devices like voltage sensors. The algorithm's execution can be seamlessly integrated into the current systems without requiring significant adjustments. Experiments and simulations for the digitally controlled PMSM drive system are conducted to demonstrate the efficacy of the suggested approach. The promising method's validity is confirmed by the modelling and experimental results, which also demonstrate its practical worth and good performance.

## Reference

- [1] P. C. Krause, O. Wasynczuk, and S. D. Sudhoff, *Analysis of Electric Machinery*, IEEE Press: IEEE Power Eng. Soc., 1995.
- [2] Liuping Wang, Shan Chai, Dae Yoo, Lu Gan, Ki Ng - PID and Predictive Control of Electrical Drives.
- [3] R. L. A. Ribeiro, C. B. Jacobina, E. R. C. Silva, and A. M. N. Lima, "Fault detection of open-switch damage in voltage-fed PWM motor drive systems," *IEEE Trans. Power Electron.*, vol. 18, no. 2, pp. 587–593, Mar. 2003.
- [5] H. Schwab, A. Klönn, S. Reck, and I. Ramesohl, "Reliability evaluation of a permanent magnet synchronous motor drive for an automotive application," in *Proc. Conf. Rec. 10th Eur. Power Electron. Appl. Conf.*, Toulouse, France, 2003, ISBN: 90-75815-07-7.
- [6] O. S. Yu, N. J. Park, and D. S. Hyun, "A novel fault detection scheme for voltage fed PWM inverter," in *Proc. IEEE Ind. Electron. Conf.*, Nov. 2006, pp. 2654–2659.